Journal of Materials Chemistry B

PAPER

View Article Online
View Journal | View Issue

Cite this: J. Mater. Chem. B, 2025, 13, 10662

Towards scalable broad-spectrum photodynamic antimicrobial textiles: synergistic effect of Rose Bengal and commercial cationic fixative on polyamide fabrics

Inés Martínez-González, [a] Pilar Moya, [b] Inmaculada Andreu, [c] Pablo Díaz García, [a] Alberto Blazquez-Moraleja, *[d] Sonia G. Delgado, [b] Ildefonso Ayala, [b] Alejandro Mateos-Pujante, [c] Marilés Bonet-Aracil, [a] M. Luisa Marin *[d] and Francisco Bosca [d]

The use of photoactive textiles to reduce infection transmission in healthcare facilities and hospitals is not on the market due to the lack of scalable and cost-effective processes to prepare these materials. To address this issue, a new photodynamic antimicrobial fabric of polyamide with Rose Bengal (RB) and a commercial cationic fixative (CF) was prepared with a simple and scalable procedure using a conventional and industrialized process for incorporating dyes into textiles. Both fabrics (with and without CF) produced more than 99% inactivation of Gram-positive and Gram-negative bacteria (*Enterococcus faecalis* and *Escherichia coli*, respectively), as well as viruses such as adenovirus rAd5. Nevertheless, it is worth highlighting that the RB fabric with CF achieved 99.9999% inactivation of *E. coli* and 99.9% inactivation of fungi such as *Candida albicans*. The study was performed upon typical indoor illumination with visible light (400–700 nm, 11.3 ± 0.2 mW cm^{-2}) during periods covering between 30 and 120 min, according to the tested microorganism. Tests performed with textiles to evaluate the persistence of the RB color in them and their capability to photosensitize the inactivation of microorganisms revealed that the CF improves the robustness of the fabric. Furthermore, the photophysical and photodynamic properties of the fabrics were evaluated by direct and indirect methods. In this context, the formation of photoactivable complexes was observed through the association of RB with CF. Moreover, it was established that the remarkable photodynamic efficiency using the fabric with CF is produced through an electron transfer from microorganisms to an excited RB–CF complex (Type I) and singlet oxygen generated from the triplet excited state of free RB (Type II).

Received 7th May 2025,
Accepted 30th July 2025

DOI: 10.1039/d5tb01089f

rsc.li/materials-b

Introduction

Microorganisms (bacteria, fungi, and viruses) showing antimicrobial resistance (AMR) have been declared by the World Health Organization (WHO) as one of the main global public health threats faced by humankind.[1] Bacterial AMR was directly responsible for 1.27 million global deaths in 2019 and contributed to 4.95 million deaths,[2] and unless adequately tackled, 10 million people a year will die from drug-resistant infections by 2050.[3] Especially relevant are those microorganisms possessing multidrug resistance (MDR) to critical classes of antibiotics, which in healthcare environments produce healthcare-associated infections (HAI), also referred to as nosocomial infections. In this context, HAIs are infections acquired while receiving health care, and they may occur in different areas of healthcare delivery, such as in hospitals, long-term care facilities, and ambulatory settings. Occupational infections that may affect staff are also considered HAIs. In the European Union, HAIs affect 6.5% of all hospitalized patients, and worldwide prevalence is likely much higher.[4]

From the above data, the need to increase health measures in healthcare environments emerges to prevent and control

[a] Departamento de Ingeniería Textil y Papelera. Escuela Politécnica Superior de Alcoy, Universitat Politècnica de València. Plaza Ferrándiz y Carbonell s/n, 03801 Alcoy, Alicante, Spain
[b] Instituto Agroforestal del Mediterráneo – Centro Ecología Química Agrícola, Universitat Politècnica de València. Avenida de los Naranjos s/n, 46022 Valencia, Spain
[c] Unidad Mixta de Investigación UPV-Instituto de Investigación Sanitaria (IIS) La Fe, Hospital Universitari i Politècnic La Fe, Avenida de Fernando Abril Martorell 106, 46026, Valencia, Spain
[d] Instituto de Tecnología Química, Universitat Politècnica de València-Consejo Superior de Investigaciones Científicas, Avenida de los Naranjos s/n, 46022 Valencia, Spain. E-mail: ablamor@itq.upv.es, marmarin@qim.upv.es

these events. Textiles in healthcare environments (curtains, bedding, clothing, *etc.*) harbor pathogens and contribute to the spread of HAIs. Despite regular cleaning, microbial contamination persists; for example, 92% of hospital curtains were found to contain pathogens within a week after cleaning.[5] In this sense, the protection of the healthcare staff and patients against hospital pathogens could be achieved with technologically adapted textile clothing to prevent infection dissemination.

The incorporation of antimicrobial products in textile fabrics has gained strength recently. Some of the latest strategies include the use of antibiotics,[6,7] cationic functionalization with quaternary ammonium salts,[8,9] graphene,[10] dendrimers,[11,12] and the use of metal nanoparticles, mainly those of silver.[13–15] However, these methods face limitations such as drug resistance, environmental toxicity, potential health risks, high costs, and limited efficacy against certain pathogens.[16]

As an alternative, antimicrobial photodynamic inactivation offers a promising approach. Photosensitizing dyes (PSDs) are able to generate reactive intermediates such as radicals and/or singlet oxygen, leading to oxidative, non-specific, and irreversible damage to microorganisms (through Type I and Type II mechanisms, respectively).[17,18] Notably, when PSDs are embedded in fabrics, the oxidative damage has always been associated with the Type II mechanism.[19] This mode of action does not typically result in resistance, as the dye remains outside the microorganism. In general, photoinactivation of Gram-positive bacteria can be achieved with any PSD, but Gram-negative bacteria usually require a cationic PSD or a combination of a neutral PSD with membrane-disrupting agents.[20] In the case of viruses, they are usually more resistant to inactivation than bacterial cells and can be easily transmitted through the air, making them harder to eliminate. Interestingly, Rose Bengal (RB, Acid Red 94) is a photosensitizing anionic dye with antimicrobial properties, showing photodynamic inactivation of SARS-CoV-2 models.[21] In this context, fabrics are ideal for antimicrobial PSDs due to their large surface area, cost-effectiveness, and easy recovery. Additionally, RB can be efficiently incorporated into textiles using conventional industrial dyeing processes. Thus, RB demonstrates antimicrobial effects in various functionalized textiles.[22–34] However, the antiviral activity against human coronaviruses has only been evaluated using high light intensities unachievable in hospital environments.[22]

Polyamide (PA) 6 is one of the textiles more widely used for fabric application due to its strength, flexibility, abrasion resistance, and thermal stability.[35–37] Its coloration with anionic dyes like RB relies on ionic interactions between the cationic protonated amino end groups of PA fabrics (PAF) and the anionic dye.[38] However, due to RB's high water solubility and poor fastness on PA, post-treatment fixation is needed to ensure durability.[39] In this context, fixatives such as quaternary ammonium salts are commonly used to enhance fastness while also providing antimicrobial properties.[38,40]

A recent antibacterial study using RB in PAF to inactivate Gram-positive bacteria has highlighted the importance of RB concentration in achieving optimal efficiency of photodynamic therapy on fabrics.[26] In fact, the aggregation of RB supposes a significant limitation that hampers light-induced reactive oxygen species (ROS) production by causing self-quenching of RB. Moreover, in this preliminary study, we showed that an RB concentration above the optimal conferred an anionic character to the RB-PAF, leading to electrostatic repulsion against Gram-positive bacteria and thereby hindering the fabric's photodynamic effect.

Hence, alternative approaches have been explored in other materials, such as using polycationic chains[23,33,41,42] or capturing RB in mesopores,[27] to avoid aggregation or improve the cationic surface area to increase bactericidal efficacy. Despite their potential, these strategies often involve synthetic protocols that are difficult to adapt to the textile industry, have high costs, or may compromise the physical properties of the fabrics.

Here, we present a novel, scalable method for creating a highly effective photosensitizing PAF with broad-spectrum antimicrobial activity. Using an industrially viable dyeing process, polyamide was functionalized with RB and a commercial cationic polymer. This innovative fabric was effective against Gram-positive and Gram-negative bacteria, fungi, and viruses using visible light with intensities suitable for hospital environments, which reinforces the potential of this approach for next-generation antimicrobial textiles. Moreover, results of mechanistic studies revealed that electron transfer processes (Type I photosensitization mechanism) must be substantially occurring in the RB antimicrobial action. Thus, we demonstrate for the first time that the Type I mechanism is involved in the photosensitized microbial inactivation by a dyed textile.

Results and discussion

Synthesis of the dyed fabrics

Fibers, such as polyamide, contain amino and carboxyl groups in the isoelectric range (pH 5.0) and are mainly ionized to NH_3^+ and COO^-. In an acid dyebath, the carboxylate ions are converted to undissociated carboxyl groups owing to the addition of acid, giving the positively charged fiber to take an equivalent amount of acid anions. Dyeing involves the exchange of the anion associated with an ammonium ion in the fiber with a dye anion. The dye anions exhibit a greater affinity for the substrate than the much smaller acid anions.[39] Polyamide fabric (PAF) dyed with Rose Bengal disodium salt (RB) will be denoted as RB-PAF.

Based on previous studies, the dyeing was carried out at the optimal RB concentration (1% o.w.f.) to achieve maximal photodynamic efficacy against Gram-positive bacteria.[26] The novelty of the coloring process is based on the use of a commercial fixative agent, a cationic quaternary polymer (CF, 0.6% o.w.f.) commonly used in the textile industry to fix direct or reactive dyes, mainly during cellulosic fiber dyeing. Herein, it is employed in the dyeing of polyamide with an anionic dye to enhance the positive charges and consequently broaden the spectrum of microorganisms targeted by the treated fabric. Thus, PAF dyed with RB (RB-PAF) was subsequently treated with the fixative to obtain CF–RB-PAF (see more details in Fig. S1).

Surface morphology analysis *via* SEM demonstrated that the fiber structure (*ca.* 10 μm) remained unchanged before and after dyeing (Fig. S2), suggesting that the interaction between RB and CF did not affect the fabric's morphology. The infrared spectrum of the fabrics (Fig. S3) exhibited key bands at 3290–3500 cm^{-1} (N–H stretching), 1630–1670 cm^{-1} (C═O stretching), 1530–1550 cm^{-1} (N–H bending and C–N stretching), and 2850–2950 cm^{-1} (–CH_2–/–CH_3 stretching).

Determination of dye concentration in wastewater. The dyeing curve has achieved a high exhaustion percentage of over 97% (Fig. S4 and Table S1). The addition of the fixative agent after dyeing does not affect the dye exhaustion process itself since it is a post-treatment. However, applying the fixative means that fewer washes are necessary to obtain a negligible dye concentration in the wastewater, which is the moment that the fabric can be considered as no longer releasing color. In addition, as expected, the dye concentration per gram of fabric is slightly higher in the fixative case, as it helps to reduce color loss during the washing process.

Determination of chromatic coordinates. Wastewater analysis (Table S1) shows minimal differences in bath exhaustion with or without the fixative, corroborated by Fig. 1 (see Fig. S5 and Table S2 for color measurements). Dyed fabrics exhibit a fuchsia tone with high red (+a*) and some blue (−b*). The fixative-treated fabric appears darker (lower L*), with more red and slightly less blue. This color difference (ΔE^* = 6.38) is visible to the naked eye. A control test confirmed that the fixative itself does not alter fabric color, indicating the observed change is due to its interaction with the dye.

Durability of the color of the fabrics (CF-)RB-PAF. Fabric sample images of the original polyamide fabric (PAF), RB-PAF, CF–RB-PAF, and its appearance after 5 cycles (CF–RB-PAF-5CW) or 10 cycles of washing (CF–RB-PAF-10CW) using the standard UNE-EN ISO 105-C06:2010 were recorded using a magnifying glass (see Fig. 1). As shown in Table S2, a moderate color difference (ΔE^* = 6.17) appears after five washes, mainly due to color loss (increased L*). However, after ten washes, the difference is minimal (ΔE^* = 6.41), indicating that most color loss occurs during the first five cycles. This suggests that further washing is unlikely to result in significant fading.

Although preliminary washes of CF–RB-PAF had already been carried out until no color loss was detected in the water, the color loss observed during the standardized first five aging washes may be attributed to differences in washing conditions. In fact, a powder detergent was used for the washing tests according to ISO standards. The detergent may be aggressive for the dye and/or the fixative (CF), even though these washes have been carried out at a moderate temperature (40 °C). Notably, the chromatic coordinates of RB-PAF (Table S2 and Fig. S5) are similar to those of aged CF–RB-PAF samples (5CW, 10CW), suggesting that the detergent may cause significant leaching of the fixative component.

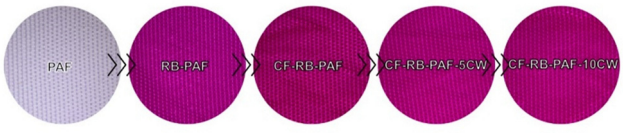

Fig. 1 Images of PAF after different treatments recorded using a magnifying glass.

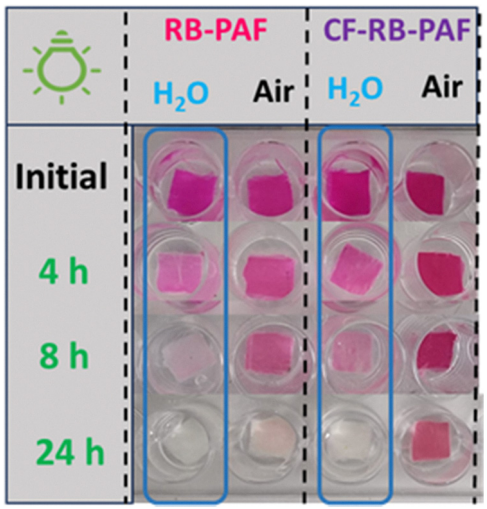

Fig. 2 Photostability of ~1 cm^2 of CF–RB-PAF and RB-PAF in aerated media, with and without the presence of water, using a white light irradiation intensity of 9 mW cm^{-2}. Real pictures were taken at the beginning and after 4, 8, and 24 hours of irradiation.

Additionally, we evaluated fabric photostability under white light (9 mW cm^{-2}) in both air and water for up to 24 hours. This irradiance closely matches the values applied in antimicrobial studies. However, it is worth noting that the photostability of the textiles is often evaluated in the literature using irradiance values more than ten times lower than those used for the antimicrobial tests.[43,44]

The higher photostability of both fabrics under air than in water can be mainly attributed to the different O_2 diffusion constants (1.98×10^{-5} m^2 s^{-1} for air *vs.* 1.90×10^{-9} m^2 s^{-1} for water)[45] that results in lower contact time between the dye and the photogenerated $^1O_2$ under air compared to aqueous media (Fig. 2). Moreover, CF–RB-PAF showed significantly slower RB photobleaching than that observed for RB-PAF. Similar photostability results were obtained when the fabrics were evaluated based on their diffuse reflectance spectra (Fig. S6).

Antimicrobial photodynamic inactivation studies

Photodynamic inactivation combines a photosensitizing agent, light at specific wavelengths, and molecular oxygen to produce reactive intermediates such as radicals and/or singlet oxygen that can kill microorganisms, including bacteria, fungi, and viruses. The study was performed using visible light (400–700 nm) with an irradiance of 11.3 ± 0.2 mW cm^{-2} (see Fig. S7). This irradiance is high for places such as rooms, but is suitable for use in enclosed spaces like hospitals.

Bactericidal activity. Bactericidal photodynamic activity of RB-polyamide fabrics with and without cationic fixative (CF–RB-PAF and RB-PAF, respectively) was evaluated under

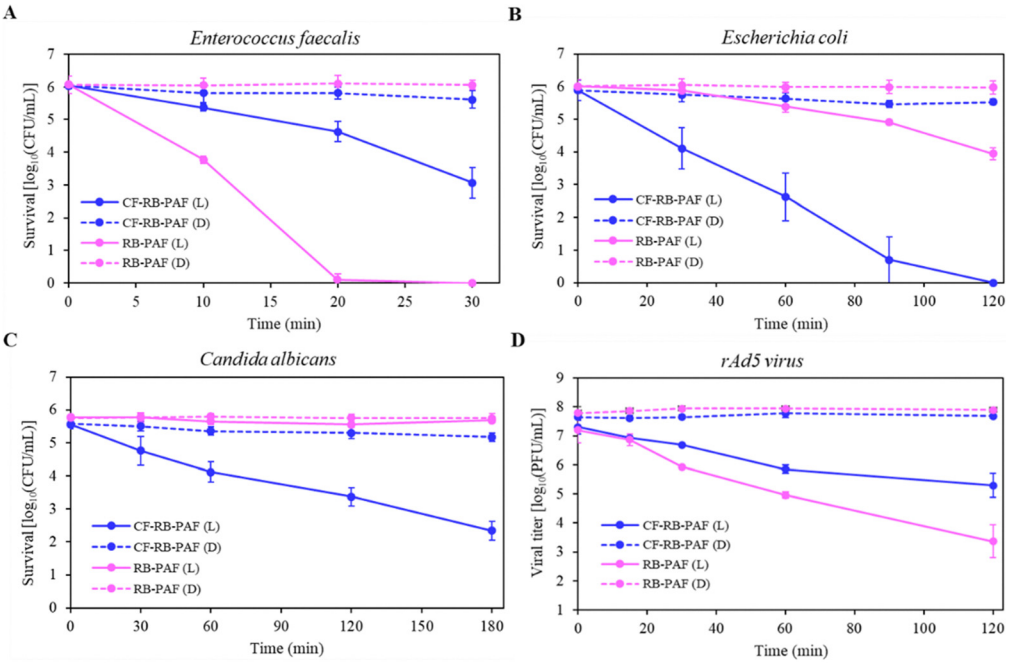

Fig. 3 Antimicrobial activity of CF–RB-PAF and RB-PAF under light exposure (L; visible light, 11.3 mW cm^{-2}) or dark conditions (D) against: (A) Gram-positive (*Enterococcus faecalis*) bacteria, (B) Gram-negative (*Escherichia coli*) bacteria, (C) *Candida albicans* fungus and (D) rAd5 virus. Data are shown as mean values ± standard error of three independent experiments performed in duplicate.

fixed illumination conditions (see Section S6 in SI) against Gram-positive (*E. faecalis*) and Gram-negative (*E. coli*) bacteria. In general, photoactive fabrics were highly efficient inactivating *E. faecalis* under illumination, while slight or negligible effects on survival were observed in dark conditions (Fig. 3A). After 10 min of light exposure, important differences in activity among the four tested groups, irradiated and non-irradiated fabrics ($F_{3,8}$ = 77.15; $P < 0.0000$), were already recorded. Thus, irradiated RB-PAF could reduce more than 2 $\log_{10}$ units of bacteria survival, this being significantly more active than irradiated CF–RB-PAF, which only induced a reduction of 0.5 $\log_{10}$ units. Despite the low activity level reached by CF–RB-PAF after 10 min of irradiation, it was high enough to be significantly different from those shown by the fabrics in dark conditions ($P < 0.05$). As exposure time to irradiation enlarged, the inactivation activity of photoactive fabrics proportionally increased, and the same statistical tendency, regarding differences among the tested groups, was revealed both at 20 min ($F_{3,8}$ = 407.35; $P < 0.0000$) and at 30 min ($F_{3,8}$ = 300.26; $P < 0.0000$). The highest photodynamic activity was shown in only 20 min by RB-PAF, which reduced bacteria survival by more than 6 $\log_{10}$ units. Because our initial bacterial concentration was around 1×10^6 ufc mL^{-1}, this reduction meant almost the fully complete inactivation, which was truly confirmed at 30 min. On the other hand, CF–RB-PAF inoculated with bacteria and irradiated showed a lesser but also important bactericidal activity, exhibiting 3 $\log_{10}$ units of survival reduction at the end of the experiment.

In addition to photoactive fabrics, PAF and CF-PAF were also evaluated against *E. faecalis*, either under light exposure or in the dark, to assess if there was any antimicrobial effect directly derived from pristine fabric or from the polyamide fabric only functionalized with CF. As expected, PAF was ineffective in inactivating *E. faecalis*, and CF-PAF activity was unimportant (0.4 $\log_{10}$ units of survival reduction at 30 min).

Contrary to what happened against *E. faecalis*, the most photoinactivating fabric against *E. coli* was CF–RB-PAF (Fig. 3B). Under irradiation, this fabric showed linear inactivation kinetics and required 120 min to reach the total killing of all bacteria (100% inactivation). At 30 min of light exposure, it exhibited a significantly higher level of photodynamic activity than the other three groups ($F_{3,8}$ = 6.20; P = 0.0175), and this significant difference was maintained up to the end of the experiment. On the other hand, the lack of CF in the RB-PAF proved a very important loss of activity. In fact, 90 min after the beginning of the illumination period, statistical analysis revealed that its activity level was still similar to that of the 2 dark controls ($P > 0.05$). Only at 120 min, irradiated RB-PAF was statistically more active (2.06 $\log_{10}$ units of survival reduction; $P < 0.05$) than the non-irradiated controls. As in the case of *E. faecalis*, PAF was ineffective in inactivating *E. coli*, and CF-PAF showed a very slight activity, reducing by 0.3 $\log_{10}$ units the viability of the bacteria in both irradiated and non-irradiated conditions. This latter activity is similar to that shown by CF–RB-PAF under dark conditions (survival reduction of 0.36 $\log_{10}$ units), and both activities would be related to the presence of the positively charged groups in our polymeric cationic fixative. It has been widely reported in the literature that cationic functionalities, such as those found in cationic polymers, can inactivate microorganisms through non-specific

mechanisms that inhibit pathogen growth, even causing bacterial lysis.[46] According to Azevedo *et al.*,[47] the biocidal performance of cationic groups begins with the adsorption of microbes onto the surface containing the cationic polymer due to electrostatic interaction between positively charged groups of the polymer and negatively charged groups of microbes' surfaces. This interaction results in an increase in cell permeability and the disruption of the cell membrane. Although the antimicrobial activity level of cationic polymers has been reported as being usually strong,[46] in our experimental conditions, the polymeric CF has only shown a weak bactericidal activity, as denoted by results arising from CF-PAF and non-irradiated CF–RB-PAF. However, it was able to strongly synergize the RB-mediated photoinactivation, as complete inhibition of *E. coli* (100% inactivation) was obtained. Two factors could contribute to producing this potent synergistic effect. Firstly, RB has been widely described as having little photodynamic effect against Gram-negative bacteria due partly to its inability to approach the negatively charged bacterial surface.[25,26,48,49] Therefore, the higher affinity of our cationized fabric to *E. coli* should have improved the bactericidal activity, as the close contact between the photosensitizer and cells leads to better photodynamic performance. Our results concerning bacterial adsorption on the fabrics clearly confirm this hypothesis, as CF–RB-PAF was 60% more efficient in attaching *E. coli* than RB-PAF (Fig. S8). These findings are consistent with results observed in previous studies using different RB-supporting materials.[23,33]

The second important factor that could be taking part in the observed synergy should be the coexistence of Type I and Type II photodynamic mechanisms generated in the presence of CF. Rose Bengal has been traditionally reported as possessing a low probability of triggering Type I photoreactions. However, under special circumstances, such as those where massive H-donors closely surround RB molecules, Type I photoreaction can also occur.[27,50] In our case, the great abundance of amino groups in the CF could provide the ideal environment around the RB molecules to produce electron transfer reactions between RB excited states and reactive amino acids of proteins of the outer membrane of Gram-negative bacteria (Type I mechanism).[51] Thus, the simultaneous occurrence of Type I and Type II pathways could combine the generation of different reactive species, which led to the improved efficiency of CF–RB-PAF against *E. coli*.

In the case of *E. faecalis*, where the adsorption of the bacteria to CF–RB-PAF and RB-PAF is quite similar (Fig. S8), the lower activity of CF–RB-PAF than that of RB-PAF could be understood taking into account the negligible reactivity of the cell components of the outer membrane of Gram-positive with RB excited states and the competitive reactivity that must take place between the added CF and the cellular components of the bacteria for the singlet oxygen generated from excitation of RB.[52,53] Overall, adsorption of CF–RB-PAF with *E. faecalis* would not produce any reaction arising from the Type I mechanism, and the Type II mechanism must produce lower membrane damage than in the case where the adsorption occurs between RB-PAF and *E. faecalis*.

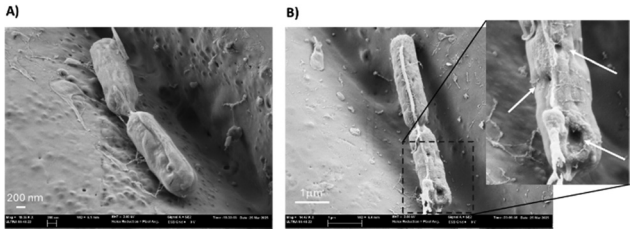

Fig. 4 Scanning electron microscopy images of *E. coli* inoculated on the photodynamic fabric CF–RB-PAF. (A) Fabric + *E. coli* + Dark; (B) Fabric + *E. coli* + Light. A partial magnification of this image shows morphological alterations in the bacterial cell wall (white arrows). Fabrics were inoculated with 10 μL of 1×10^8 bacteria per mL and a white light (11.3 mW cm^{-2}) was used for 90 min in the irradiated sample.

According to the literature, the cell wall is the main target of the RB photodynamic activity, which is the photooxidation of structural components, thereby leading to the leakage of cell content. In order to evidence bacterial cell damage caused by the photodynamic fabrics, cryo-SEM studies were performed (Fig. 4 and Fig. S9). Thus, after performing the bacterial photoinactivation with the photoactive fabrics, samples were analyzed by SEM. Thus, the images confirmed intense morphological alteration of the bacteria's walls. In the case of *E. coli*, as it is shown in Fig. 4 and Fig. S9, death cells of *E. coli* typically showed invagination zones in their wall, from which the leakage of cell content, as described, is likely to occur. A loss of morphological integrity in the shape of *E. faecalis* was also observed (Fig. S9).

Fungicidal activity. The yeast *C. albicans* was also notably inactivated by irradiated CF–RB-PAF (Fig. 3C), which was able to significantly reduce the concentration of viable cells, compared to the other three treatments, from 60 min of irradiation ($F_{3,8}$ = 18.54; P = 0.001). Furthermore, at the end of the experiment, it was able to reach almost 3 $\log_{10}$ units of viability reduction. Although this level of fungal inactivation can be considered an important activity, mainly considering the scarce photoactivity of RB against *C. albicans* previously reported,[41,54] the time required to reach inactivation was as long as 180 min, which is consistent with the lesser susceptibility of this microorganism to photodynamic inactivation. According to Donnelly *et al.*,[55] unlike prokaryotic bacteria, *C. albicans* is harder to photoinactivate because it is a larger and more complex eukaryotic fungus, so exposure to higher RB concentrations and stronger light doses would be likely required to control this fungus. On the other hand, in dark conditions, CF–RB-PAF induced a viability reduction of 0.4 $\log_{10}$ units. Similar to what happened against bacteria, this activity would be connected with the presence of the cationic fixative, considering that fungal inactivation has also been previously reported from materials containing polycationic groups, such as those found in ammonium compounds.[56]

Viricidal activity. To investigate the antiviral activity of the polyamide fabrics RB-PAF and CF–RB-PAF upon irradiation with visible light, the plaque assay was employed using a recombinant adenovirus vector type 5 (rAd5) as a virus model.

Thus, in the former stage, we assessed the infectivity of the viral vector in both HEK-293 and A549 cells using the β-Galactosidase (βGal) activity assay. This assay was employed because the viral vector contains the *E. coli* LacZ gene, encoding the βGal enzyme, widely utilized as a reporter for gene expression.[57] In this context, cells were seeded in two 96-well plates and infected with a ten-fold serial dilution of a viral stock dilution (1×10^8 PFU per mL) ranging from 10^{-1} to 10^{-7}. After treatment with the β-Galactosidase assay reagent, absorbance values were recorded at 405 nm. Furthermore, the βGal expression was visually detectable by the naked eye due to a color change from non-colored to yellow. Thus, significant overexpression of βGal was observed in HEK-293 cells, which surpassed the absorbance upper limit detectable by the microplate reader. In contrast, with A549 cells, βGal expression was minimal even in the non-stock diluted (10-0), indicating a lack of compatibility between A549 cells and the viral vector (Fig. S10). Therefore, the HEK-293 cell line was selected for evaluating the virucidal activity of the polyamide fabrics, taking advantage of the βGal overexpression.

After that, the next step was to determine the viricidal activity of the photoactive materials prepared. For this purpose, sterilized fabrics were exposed to 100 μL of a viral stock dilution (1×10^8 PFU per mL) and either irradiated to increased irradiation times (15, 30, 60, 120 min) or kept in the incubator for the same time in 24-well plates (dark conditions). It is important to note that, for both dark and visible light conditions, a well plate with the virus alone was employed as the negative control, respectively. Subsequently, viruses from all conditions were recovered, and their viral titers were determined according to the plaque assay, where HEK-293 cell culture monolayers were infected with ten-fold serial dilutions for each condition. Following an 8-day incubation to allow the formation of clearly countable plaques, viral titers were then calculated through visual scoring of all foci. Representative images of the plaque assay are shown in Fig. S11.

As observed in Fig. 3D, the highest reduction in the viral titer was achieved in the RB-PAF, resulting in a 4 log10 reduction in the titer after 120 min of irradiation. Conversely, in the presence of the fixative (CF–RB-PAF), this reduction decreases to 2 $\log_{10}$ of viricidal activity, pointing out that the presence of the cationic fixative reduces the viricidal activity of the polyamide fabric dyed with RB. This fact could be attributed to the repulsive effect of the cationic textile on these microorganisms. This effect may be produced due to both types of microorganisms having positively charged regions on their surfaces. In this context, the surface of CF–RB-PAF has a large number of cations. Although in CF–RB-PAF, the percentage of CF is *ca.* 0.6% and that of RB is *ca.* 1%, the molecular ratio between them in the fabric is 3/1 CF/RB. Thereby, as each monomer of CF must have more than 4 cations before being added to the textile, while RB in the textile has only one anion, there is a large excess of cations and, accordingly, of CF to neutralize the anionic charge of RB. Thus, a decrease in the amount of CF in RB-PAF could maintain the antimicrobial activity against Gram-negative bacteria and fungi and increase it against Gram-positive bacteria and viruses.

In this sense, other studies have observed that polyester, cotton, and silk coated with photo-cross-linked polymers with cationic charges containing RB have higher antiviral activity against adenovirus, but using visible light at an irradiance *ca.* 6 times higher than the one applied in the present study.[22,44] In fact, the irradiance of those studies (65 mW cm^{-2}) is too high to be used in closed spaces such as hospitals. This value is roughly half of the solar constant (137 mW cm^{-2}), which represents the solar irradiance at noon with the Sun directly overhead.

Durability of antimicrobial activity of the photoactive fabric CF–RB-PAF. Based on the broad spectrum of antibacterial activity exhibited by photoactive CF–RB-PAF, this fabric was selected to assess if washings could affect its long-term use in practical applications. Thereby, as is shown in Fig. 5, the bacterial inactivation kinetics of the CF–RB-PAF-10CW were compared to those obtained for the fabric before the washings (CF–RB-PAF). The efficiency of the washed fabric in inactivating *E. coli* was considerably reduced as a loss of activity of approximately 3 $\log_{10}$ units was found at the end of the experiment (Fig. 5B). On the other hand, washed fabric notably increased its photocatalytic activity against *E. faecalis* in such a way within 15 min of irradiation, it was able to reduce 3.5 $\log_{10}$ units more the bacteria viability than the non-washed CF–RB-PAF (Fig. 5A). Obtained results, both against *E. coli* and *E. faecalis*, would be compatible with a loss of cationic fixative due to the washings. According to the behavior previously showcased when RB-PAF and CF–RB-PAF without washings were compared, this hypothesis could justify the deterioration of activity against *E. coli* and the improvement against *E. faecalis.*

Although the activity level remaining in the aged fabric is still highly relevant after 10 washing cycles, this feature may be easily improved by optimizing the RB and CF rates and concentrations to make the fabric more durable and long-lasting. In this sense, long-term antibacterial washing-based durability without activity loss after 30 washings has been recently reported from a fabric developed using RB on cotton-based super-adsorptive fibrous equipment.[27]

The antifungal activity of aged fabric was evaluated under the same conditions as non-aged fabric. Thus, after 10 washing cycles, CF–RB-PAF-10CW was completely inefficient against *C. albicans*. Given this result, the 5 washing cycles sample CF–RB-PAF-5CW was also evaluated, but the same finding was achieved (Fig. 5C), which points out a very quick loss of photodynamic activity. This finding aligns with the lower susceptibility of this organism to photodynamic action, as previously noted, and the loss of positive charges during the washing process. Based on these results, CF–RB-PAF serves as a promising starting point for further practical developments with antifungal activity, but significant improvements are necessary. In fact, other studies of RB in textiles have shown that when they are coated with photo-cross-linked polymers containing this dye, the antimicrobial activity is better.[44]

Regarding the durability of the viricidal efficacy of the photoactive fabric, the viricidal activity of the samples was assessed using the plaque assay. As depicted in Fig. 5 and Fig. S12, there is a significant enhancement in the antiviral

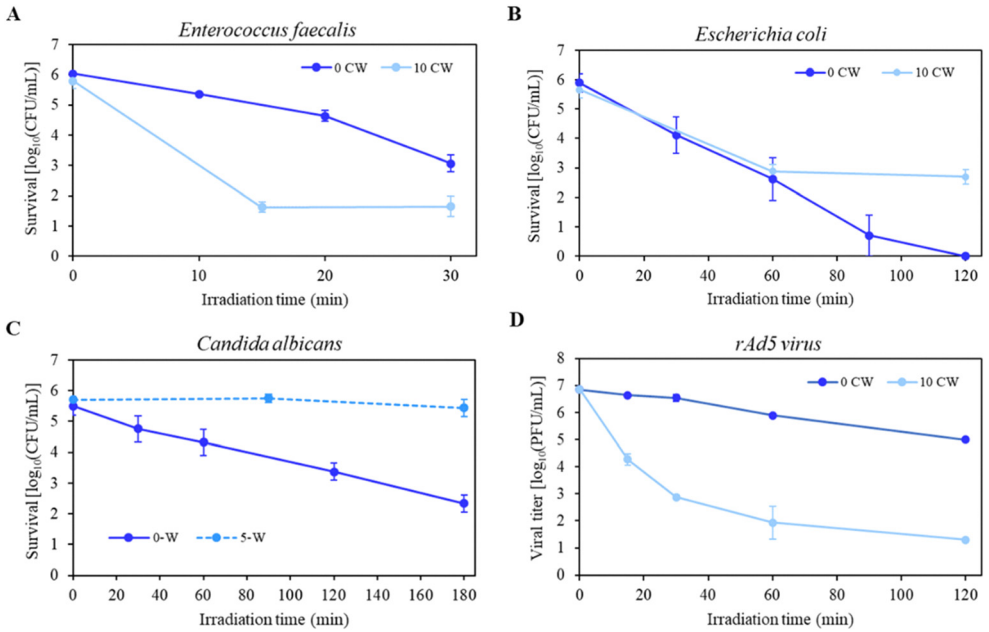

Fig. 5 Effect of washings on the durability of the antimicrobial photodynamic activity of CF–RB-PAF against (A) Gram-positive (*Enterococcus faecalis*) bacteria, (B) Gram-negative (*Escherichia coli*) bacteria, (C) *Candida albicans* fungus and (D) rAd5 viral titers in HEK-293 cells after irradiation of a viral stock solution (1×10^8 PFU per mL) over polyamide fabrics at different irradiation times (15, 30, 60, 120 min). Data corresponding to 10 or 5 washing cycles (CW) are represented as mean values ± standard error from 5 or 4 independent replicates for bacteria or fungus, respectively. For the virus, data corresponding to 10CW are represented by mean ± SD of three independent experiments performed in duplicate.

activity of the washed polyamide fabric CF–RB-PAF compared to the unwashed fabric, with an increase of more than 2 $\log_{10}$ of viricidal activity. This outcome could be attributed to a reduction in the positive charges provided by the cationic fixative after washing, resulting in behavior like the CF-untreated polyamide fabric (RB-PAF), which exhibited viricidal activity of the same magnitude (see Fig. 5).

Photophysical properties of CF–RB-PAF and RB-PAF

The electrostatic interactions between the protonated amino groups of the fixative and the deprotonated phenol and carboxyl groups of the dye could be anticipated to form complexes. In trying to understand the relevant antimicrobial differences observed in the RB fabrics when the cationic fixative is added, deep photophysical characterization of CF–RB-PAF and RB-PAF was performed. In fact, some RB photophysical properties could be altered in the fabric when cationic fixative is added.

For instance, the diffuse reflectance spectra of CF–RB-PAF and RB-PAF (Fig. 6A) reveal a bathochromic shift due to the cationic fixative treatment. Specifically, CF–RB-PAF shows three peaks (520, 547, and 582 nm), while RB-PAF presents only two (525 and 560 nm). This shift cannot be caused by dye aggregation, which would reduce antimicrobial activity.[27] A similar decrease in RB absorption intensity, together with a ~10 nm bathochromic shift, was observed when increasing fixative concentrations were added to an aqueous RB solution (Fig. 7A), suggesting that CF modifies RB's molecular environment through electrostatic interactions with its phenol and carboxyl groups.[58]

With the aim of elucidating the impact of the cationic fixative on the photophysical characteristics of the dyed polyamide fabrics, steady-state and time-resolved emission measurements, laser photolysis experiments (LFP), and singlet oxygen ($^1O_2$) generation were conducted. Steady-state fluorescence spectra of CF–RB-PAF and RB-PAF show a bathochromic shift (*ca.* 40 nm) compared to the emission of the homogeneous RB (λ_{max} = 568 nm) in aqueous medium (Fig. 6B).[23,24,26,59] The influence of the CF on the first singlet excited state of RB was also investigated under homogeneous conditions. In this case (Fig. 7B), the addition of increasing concentrations of CF to aqueous RB results in the quenching of RB fluorescence. A Stern–Volmer fluorescence quenching constant value of 1.2×10^5 M^{-1} was determined. This high value agrees with the anticipated formation of a complex between CF and RB (CF–RB). Dynamic fluorescence quenching of ^{1}RB* by CF was discarded since the fluorescence lifetime (τ_F) of RB does not decrease in the presence of the cationic fixative (more details in Fig. S13). The resulting complex exhibits a slightly different emission maximum (λ_{max} *ca.* 580 nm); see pink and green traces in Fig. 7B.

Laser flash photolysis (LFP) studies were also conducted on the fabrics to track the formation of the triplet excited state of RB (^{3}RB*), which is critical for predicting singlet oxygen generation. Transient absorption spectra (TAS) of CF–RB-PAF and RB-PAF were recorded at various time intervals after the laser pulse, with an excitation wavelength of 532 nm under air employing a spectral detection range of 300 to 800 nm (Fig. 6C for CF–RB-PAF and Fig. S14 for RB-PAF). The TAS of both fabrics was identical, with prominent absorption peaks at *ca.* 380, 475, and 625 nm and a bleaching band centered at *ca.* 540 nm with comparable lifetimes in aerated and deaerated

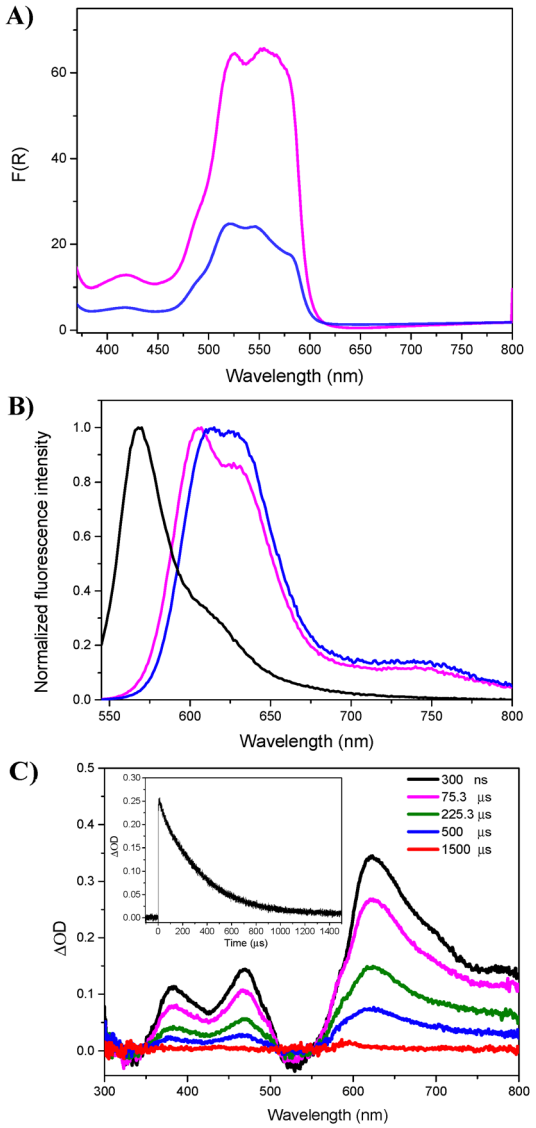

Fig. 6 (A) Diffuse reflectance spectra of CF–RB-PAF (blue) and RB-PAF (pink). (B) Normalized steady-state fluorescence emission spectra obtained under aerobic conditions from CF–RB-PAF (blue) and RB-PAF (pink) and from aqueous solution (6.6 μM) of RB (black). The excitation wavelength (λ_{exc}) for heterogeneous was 550 nm and 520 nm for homogeneous medium. (C) Transient absorption spectra of CF–RB-PAF recorded at different times after the laser pulse (λ_{exc} = 532 nm in aerated media). Inset: Trace recorded at 600 nm.

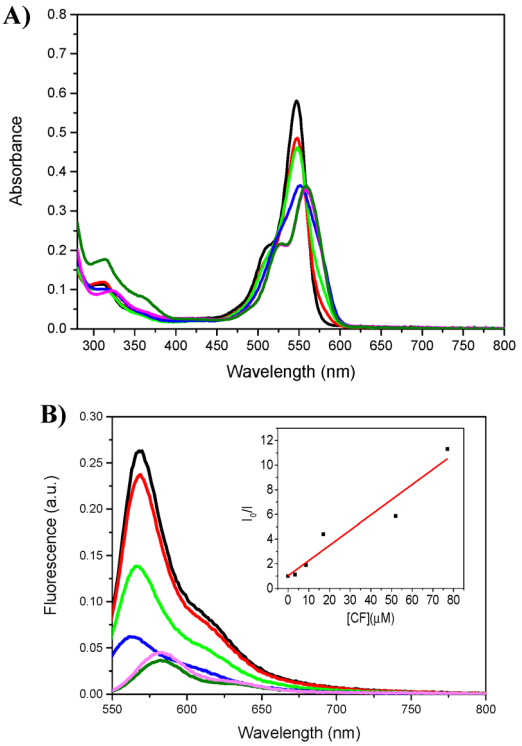

Fig. 7 (A) Absorption spectra of an RB (6.6 μM) aqueous solution at pH 5.7 in the absence (black) and in the presence of different concentrations of CF: 3.4 (red), 8.6 (green), 17 (blue), 52 (pink), and 77 μM (dark green). (B) Emission spectra generated from the above RB aqueous solutions. Inset: Corresponding Stern–Volmer plot recorded at 568 nm.

media (340 μs and 353 μs for CF–RB-PAF and RB-PAF, respectively). It is well-known that ^{3}RB* is quenched efficiently by O_2 under homogeneous conditions; quenching constant values close to diffusion control have previously been reported in various solvents.[60,61] In a previous report,[26] we unambiguously assigned for the first time the bands observed in the TAS of a polyamide fabric dyed with RB to the ^{3}RB* based on the correlation of the fading of these signals to the disappearance of its phosphorescence. Thereby, we safely assume that the TAS detected in CF–RB-PAF and RB-PAF is due to ^{3}RB* generated from the free RB ground state.

To shed more light on the formation of the putative complex CF–RB, we also analyzed the behavior of ^{3}RB* *versus* the cationic fixative under deaerated homogeneous conditions. Thus, it was observed that ^{3}RB* lifetime does not decrease with increasing concentrations of the cationic fixative (Fig. S15). However, the intensity of the signals decreased till the complete quenching of the signal was achieved after adding 77 μM CF (Fig. S15B). Using the Stern–Volmer equation with the intensity of the ^{3}RB* signal at 600 nm *vs.* CF concentrations, a quenching constant value of 1.6×10^5 M^{-1} was determined, which was very similar to the determined one using the steady-state fluorescence quenching of RB by CF. In fact, both data show the same effect, less generation of the excited states of RB by the addition of CF, in agreement with the formation of the CF–RB complex. Further evidence of the complexation of RB ground state with CF in the fabrics was obtained from NMR experiments, where increasing the concentration of CF caused the disappearance of the characteristic RB signals in ^{1}H and ^{13}C NMR (see more details in SI and Fig. S16).

The singlet oxygen generation from the fabrics was monitored through the characteristic singlet-oxygen phosphorescence at λ = 1270 nm induced by a pulsed laser in aerated media. Hence, we detected a similar intensity of $^1O_2$ generation from CF–RB-PAF and RB-PAF (Fig. S17A). Moreover, these decays revealed a lifetime of the generated $^1O_2$ very similar for both fabrics (*ca.* 190 μs). Thus, the singlet oxygen generation

detected in both textiles ought to be produced from the excitation of the free RB moieties. In fact, the non-singlet oxygen generation from the putative complex CF–RB was clearly evidenced when the signal at 1270 nm generated in homogeneous solutions of RB disappeared upon CF addition (Fig. S17B).

Accordingly, these results indicate that in CF–RB-PAF, not all the RB chromophores are forming complexes with the CF.

The photophysical studies performed with the fabrics have evidenced that RB-PAF has only free RB moieties, while CF–RB-PAF contains free RB molecules and CF–RB complexes. Consequently, besides assessing the effect of the $^1O_2$ generated in the fabrics (Type II mechanism), we tried to prove the involvement of Type I mechanism after excitation of the CF–RB complexes of the fabric. To achieve this, we added increasing concentrations of a negatively charged molecule with electron-donating properties to an aqueous solution of RB complexed with CF. For this purpose, we selected 9,10-anthracene dicarboxylic acid (DAA). This molecule serves as a model for the negatively charged, electron-rich amino acids commonly found in membrane proteins of microorganisms. Since the CF–RB complex exhibits fluorescence emission, steady-state fluorescence measurements were performed upon the addition of DAA to the CF–RB solution. A clear quenching of fluorescence was observed, indicating a strong interaction between DAA and the CF–RB complex (Fig. 8). In contrast, control experiments performed in the absence of CF showed only a weak interaction between RB and DAA (Fig. S18). In fact, Stern–Volmer constants of the fluorescence quenching assays revealed a value of 4.2×10^4 M^{-1} for DAA/CF–RB, while for DAA/RB it was only 6.6×10^2 M^{-1}. These results can be directly correlated with the corresponding association constants, since the fluorescence lifetimes of both CF–RB and free RB are too short for the observed emission decrease to be due to a dynamic quenching process. Therefore, although electron transfer from DAA to the singlet excited state of CF–RB or RB can occur, the process is significantly more efficient in the case of CF–RB, consistent with the DAA/CF–RB association constant being *ca.* 100 times greater than that of DAA/RB. This result provides strong evidence supporting that the excited state of CF–RB can undergo electron transfer with donor molecules and, by extension, that CF–RB-PAF can interact with electron-donating biomolecules *via* a Type I photochemical mechanism.

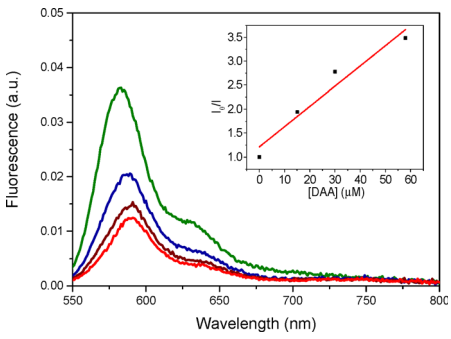

Fig. 8 Quenching of the fluorescence emission of an aqueous mixture of RB (6.6 μM) and CF (77 μM) at pH 5.9 (dark green) upon the addition of increasing concentrations of 9,10-anthracene dicarboxylic acid (DAA): 15 μM (blue), 30 μM (brown), and 58 μM (red).

Although the generation of singlet oxygen ($^1O_2$) from both fabrics was confirmed *via* direct phosphorescence emission, an indirect chemical method was applied to quantify $^1O_2$ production from CF–RB-PAF and RB-PAF. This approach, based on the photooxidation of 9,10-dimethylanthracene (DMA) monitored by absorbance decrease, revealed that, surprisingly, CF–RB-PAF induced more efficient DMA oxidation than RB-PAF (Fig. S19). Thus, we decided to perform a study of DMA photodegradation in the absence of oxygen because electron transfer reactions between CF–RB and DMA could also produce DMA degradation. Results revealed that at least *ca.* 30% of the degradation of DMA under aerated conditions could be attributed to an electron transfer (Fig. S20). Moreover, as expected, DMA degradation was insignificant with RB-PAF under anaerobic conditions. Hence, this study clearly demonstrates that the Type II mechanism involving $^1O_2$ generated from $^3RB^*$ operates in both textiles. However, in CF–RB-PAF, an additional Type I mechanism involving mainly an electron transfer between DMA and $^1(CF–RB)^*$ also takes place.

Further photodegradation tests with DMA demonstrated that the fixative significantly improved fabric reusability. CF–RB-PAF maintained effectiveness beyond 12 cycles, whereas RB-PAF lost efficiency after just 5 cycles (Fig. S21). This suggests that CF–RB complexation enhances photosensitization and increases RB photostability compared to free RB in RB-PAF.

Scheme 1 illustrates the Type I and Type II mechanisms involved in the antibacterial activity of RB-dyed textiles with and without CF. Type II arises from an energy transfer from the triplet excited state of free RB in the textiles to molecular oxygen to generate singlet oxygen. In the case of RB-PAF, Type II is the main mechanism involved. The results obtained with CF–RB-PAF can be explained by the participation of both types of mechanisms. Type I arises from the electron transfer process between the singlet excited state of the CF–RB complex and the associated negatively charged biomolecules of microorganisms' walls.

It is important to highlight that, prior to our study, only one report had proposed the coexistence of both mechanisms in the biocidal activity of functionalized textiles.[27] However, this hypothesis was based on very poor indirect pieces of evidence.

The higher photostability in the presence of CF aligns with the results observed in the heterogeneous assays (Fig. 2 and Fig. S6).

Conclusions

A new photodynamic antimicrobial fabric of polyamide with Rose Bengal (RB) and a commercial cationic fixative (CF) was prepared using a conventional, industrialized, and scalable procedure for incorporating anionic dyes into textiles. The dyeing process achieves high color intensity, high exhaustion performance, and good color fastness to washing, which is enhanced by the fixative. A thorough study of the new material was performed with and without the addition of CF to evaluate

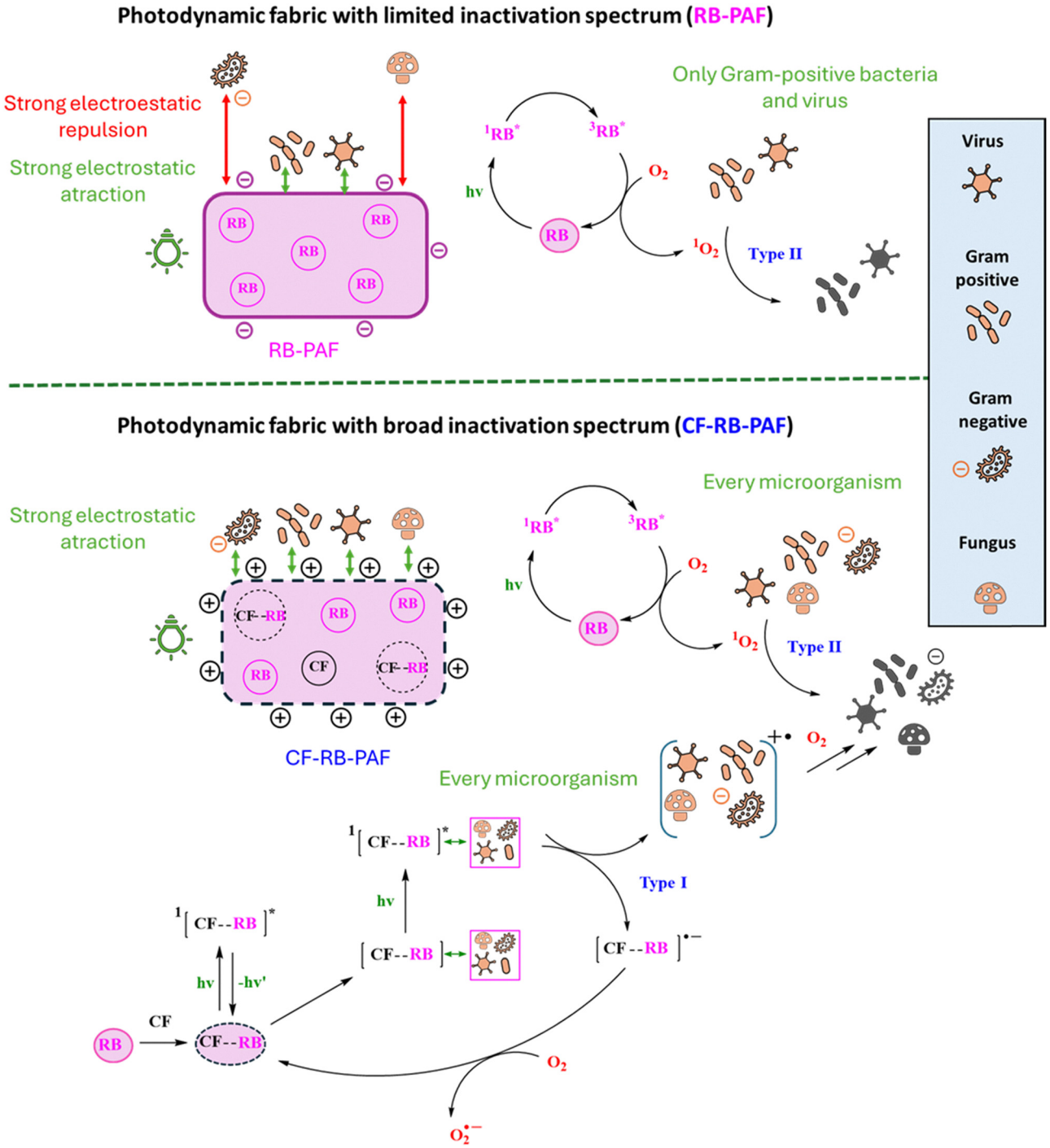

Scheme 1 Proposed mechanisms for photoinactivation of microorganisms in the fabrics RB-PAF and CF–RB-PAF.

its effect on the photodynamic properties of the polyamide. Thus, both fabrics demonstrated photosensitized inactivation to microorganisms, including Gram-positive and Gram-negative bacteria (*Enterococcus faecalis*, *Escherichia coli*, respectively), as well as viruses like *adenovirus rAd5*. However, they showed different photodynamic efficiency depending on the affinity of the material to the surface of the microorganism. In the case of studies performed with fungi such as *Candida albicans*, its inactivation was only observed when the CF was present. Furthermore, it was established that the remarkable photodynamic efficiency observed against a broad spectrum of microorganisms using the fabric with CF (CF–RB-PAF) is produced through the involvement not only of the Type II mechanism, as occurs with RB-PAF, but also of the Type I mechanism. Type I arises from an electron transfer process between the singlet excited state of a complex formed by RB and CF and

negatively charged target biomolecules of the microorganisms. In the case of Type II, singlet oxygen is generated from an energy transfer from the triplet-excited state of free RB to molecular oxygen. Thereby, the results shown in this study have revealed that the presence of CF in textiles not only changes their affinity to microorganisms but also their photodynamic behavior. Thus, next-generation antimicrobial dyed textiles can be designed with enhanced photodynamic properties, broadening their range of microorganism inactivation.

Conflicts of interest

There are no conflicts to declare.

Data availability

The data that support the findings of this study are available in the SI of this article.

The SI includes several key components, beginning with the chemicals and microorganisms used, followed by the dyeing procedure of polyamide fabrics with RB; details of the characterization of polyamide fabrics, the evaluation of the washing durability of photoactive polyamide fabric, and the assessment of the photostability of fabrics. Details of the photodynamic antibacterial and antifungal tests conducted, along with the evaluation of the capability of the functionalized fabrics to adsorb bacteria are shown. The work also includes scanning electron microscopy (SEM) and CryoSEM analyses, cell culture experiments to assess viricidal activity, and thorough data analysis. Furthermore, additional photophysical, spectroscopical, and photochemical experiments are carried out. See DOI: https://doi.org/10.1039/d5tb01089f

Acknowledgements

The authors would like to express their gratitude to the Research and Development Grants Programme (PAID-01-22) of the Universitat Politècnica de València for the contract as a pre-doctoral researcher in training (Inés Martínez-González), and are also grateful to the Agencia Valenciana de Innovacion for the funding on the strategic projects in cooperation, reference INNEST/2021/75, INNEST/2021/28 and the Conselleria de Innovación, Universidades, Ciencia y Sociedad Digital for CIAPOT/2021/33 to contract P. Norina. We also extend our gratitude to the Generalitat Valenciana and the European Union for co-funding the A.B.M. postdoctoral contract (CIAPOS/2023/201) through the European Social Fund Plus Operational Program 2021-2027 (FSE +). We would also like to extend our thanks to the Spanish Ministry of Science, Innovation and Universities and the State Research Agency (TED2021-131952B-I00 funded by MCIN/AEI/10.13039/501100011033), European Union NextGenerationEU/PRTR. Financial support by the Spanish Ministry of Science and Innovation (CEX2021-001230-S grant funded by MCIN/AEI/10.13039/501100011033) is also gratefully acknowledged.

Notes and references

1 WHO, Antimicrobial resistance, 2023, Antimicrobial resistance, 2023. https://www.who.int/news-room/fact-sheets/antimicrobial-resistance, (accessed 11 May 2024).
2 C. J. L. Murray, K. S. Ikuta, F. Sharara, L. Swetschinski, G. Robles Aguilar, A. Gray, C. Han, C. Bisignano, P. Rao, E. Wool, S. C. Johnson, A. J. Browne, M. G. Chipeta, F. Fell, S. Hackett, G. Haines-Woodhouse, B. H. Kashef Hamadani, E. A. P. Kumaran, B. McManigal, S. Achalapong, R. Agarwal, S. Akech, S. Albertson, J. Amuasi, J. Andrews, A. Aravkin, E. Ashley, F.-X. Babin, F. Bailey, S. Baker, B. Basnyat, A. Bekker, R. Bender, J. A. Berkley, A. Bethou, J. Bielicki, S. Boonkasidecha, J. Bukosia, C. Carvalheiro, C. Castañeda-Orjuela, V. Chansamouth, S. Chaurasia, S. Chiurchiù, F. Chowdhury, R. Clotaire Donatien, A. J. Cook, B. Cooper, T. R. Cressey, E. Criollo-Mora, M. Cunningham, S. Darboe, N. P. J. Day, M. De Luca, K. Dokova, A. Dramowski, S. J. Dunachie, T. Duong Bich, T. Eckmanns, D. Eibach, A. Emami, N. Feasey, N. Fisher-Pearson, K. Forrest, C. Garcia, D. Garrett, P. Gastmeier, A. Z. Giref, R. C. Greer, V. Gupta, S. Haller, A. Haselbeck, S. I. Hay, M. Holm, S. Hopkins, Y. Hsia, K. C. Iregbu, J. Jacobs, D. Jarovsky, F. Javanmardi, A. W. J. Jenney, M. Khorana, S. Khusuwan, N. Kissoon, E. Kobeissi, T. Kostyanev, F. Krapp, R. Krumkamp, A. Kumar, H. H. Kyu, C. Lim, K. Lim, D. Limmathurotsakul, M. J. Loftus, M. Lunn, J. Ma, A. Manoharan, F. Marks, J. May, M. Mayxay, N. Mturi, T. Munera-Huertas, P. Musicha, L. A. Musila, M. M. Mussi-Pinhata, R. N. Naidu, T. Nakamura, R. Nanavati, S. Nangia, P. Newton, C. Ngoun, A. Novotney, D. Nwakanma, C. W. Obiero, T. J. Ochoa, A. Olivas-Martinez, P. Olliaro, E. Ooko, E. Ortiz-Brizuela, P. Ounchanum, G. D. Pak, J. L. Paredes, A. Y. Peleg, C. Perrone, T. Phe, K. Phommasone, N. Plakkal, A. Ponce-de-Leon, M. Raad, T. Ramdin, S. Rattanavong, A. Riddell, T. Roberts, J. V. Robotham, A. Roca, V. D. Rosenthal, K. E. Rudd, N. Russell, H. S. Sader, W. Saengchan, J. Schnall, J. A. G. Scott, S. Seekaew, M. Sharland, M. Shivamallappa, J. Sifuentes-Osornio, A. J. Simpson, N. Steenkeste, A. J. Stewardson, T. Stoeva, N. Tasak, A. Thaiprakong, G. Thwaites, C. Tigoi, C. Turner, P. Turner, H. R. van Doorn, S. Velaphi, A. Vongpradith, M. Vongsouvath, H. Vu, T. Walsh, J. L. Walson, S. Waner, T. Wangrangsimakul, P. Wannapinij, T. Wozniak, T. E. M. W. Young Sharma, K. C. Yu, P. Zheng, B. Sartorius, A. D. Lopez, A. Stergachis, C. Moore, C. Dolecek and M. Naghavi, *Lancet*, 2022, **399**, 629–655.
3 P. Dadgostar, *Infect. Drug Resist.*, 2019, **12**, 3903–3910.
4 C. Suetens, K. Latour, T. Kärki, E. Ricchizzi, P. Kinross, M. L. Moro, B. Jans, S. Hopkins, S. Hansen, O. Lyytikäinen, J. Reilly, A. Deptula, W. Zingg, D. Plachouras and D. L. Monnet, *Eurosurveillance*, 2018, **23**, 1800516.
5 M. Burden, L. Cervantes, D. Weed, A. Keniston, C. S. Price and R. K. Albert, *J. Hosp. Med.*, 2011, **6**, 177–182.
6 B. M. Eid, G. M. El-Sayed, H. M. Ibrahim and N. H. Habib, *Fibers Polym.*, 2019, **20**, 2297–2309.

7 L. Rong, D. Yang, B. Wang, D. Xiao, M. Lu, Z. Mao, H. Xu, Y. Gu, X. Feng and X. Sui, *ACS Biomater. Sci. Eng.*, 2020, **6**, 3868–3877.
8 R. Oliwa, *Materials*, 2020, **13**, 3726.
9 T. Zhang, J. Gu, X. Liu, D. Wei, H. Zhou, H. Xiao, Z. Zhang, H. Yu and S. Chen, *Mater. Sci. Eng., C*, 2020, **111**, 110855.
10 S. Bhattacharjee, C. R. Macintyre, X. Wen, P. Bahl, U. Kumar, A. A. Chughtai and R. Joshi, *Carbon*, 2020, **166**, 148–163.
11 S. García-Gallego, G. Franci, A. Falanga, R. Gómez, V. Folliero, S. Galdiero, F. De la Mata and M. Galdiero, *Molecules*, 2017, **22**, 1581.
12 I. Grabchev, E. Vasileva-Tonkova, D. Staneva, P. Bosch, R. Kukeva and R. Stoyanova, *New J. Chem.*, 2018, **42**, 7853–7862.
13 Y. Wu, Y. Yang, Z. Zhang, Z. Wang, Y. Zhao and L. Sun, *Text. Res. J.*, 2019, **89**, 867–880.
14 P. OhadiFar, S. Shahidi and D. Dorranian, *J. Nat. Fibers*, 2020, **17**, 1295–1306.
15 M. A. El-Bendary, S. S. Afifi, M. E. Moharam, S. M. Abo El-Ola, A. Salama, E. A. Omara, M. N. F. Shaheen, A. A. Hamed and N. A. Gawdat, *Prep. Biochem. Biotechnol.*, 2021, **51**, 54–68.
16 *Smart Composite Coatings and Membranes. Transport, Structural, Environmental and Energy Applications*, ed. M. F. Montemor, Woodhead Publishing, Elsevier Ltd, 2016, ISBN 978-1-78242-283-9.
17 H. Abrahamse and M. R. Hamblin, *Biochem. J.*, 2016, **473**, 347–364.
18 B. Ran, L. Ran, Z. Wang, J. Liao, D. Li, K. Chen, W. Cai, J. Hou and X. Peng, *Chem. Rev.*, 2023, **123**, 12371–12430.
19 W. Chen, W. Wang, X. Ge, Q. Wei, R. A. Ghiladi and Q. Wang, *Fibers Polym.*, 2018, **19**, 1687–1693.
20 M. Q. Mesquita, C. J. Dias, M. G. P. M. S. Neves, A. Almeida and M. A. F. Faustino, *Molecules*, 2018, **23**, 2424.
21 M. Sadraeian, L. Zhang, F. Aavani, E. Biazar and D. Jin, *Mater. Today Phys.*, 2022, **28**, 100882.
22 T. Wright, M. Vlok, T. Shapira, A. D. Olmstead, F. Jean and M. O. Wolf, *ACS Appl. Mater. Interfaces*, 2022, **14**, 49–56.
23 A. Blázquez-Moraleja, P. Moya, M. L. Marin and F. Bosca, *Catal. Today*, 2023, **413–415**, 113948.
24 A. Hernández-Zanoletty, I. Oller, M. I. Polo-López, A. Blazquez-Moraleja, J. Flores, M. Luisa Marín, F. Boscá and S. Malato, *Catal. Today*, 2023, **413–415**, 113941.
25 J. Flores, P. Moya, F. Bosca and M. L. Marin, *Catal. Today*, 2023, **413–415**, 113994.
26 J. Flores, A. Blázquez-Moraleja, M. Bonet-Aracil, P. Moya, F. Bosca and M. L. Marin, *J. Environ. Chem. Eng.*, 2023, **11**, 110639.
27 P. Tang, A. Y. El-Moghazy, B. Ji, N. Nitin and G. Sun, *Mater. Adv.*, 2021, **2**, 3569–3578.
28 F. Jin, S. Liao, Q. Wang, H. Shen, C. Jiang, J. Zhang, Q. Wei and R. A. Ghiladi, *Appl. Surf. Sci.*, 2022, **587**, 152737.
29 W. Chen, J. Chen, L. Li, X. Wang, Q. Wei, R. A. Ghiladi and Q. Wang, *ACS Appl. Mater. Interfaces*, 2019, **11**, 29557–29568.
30 T. Zhang, H. Yu, J. Li, H. Song, S. Wang, Z. Zhang and S. Chen, *Mater. Today Phys.*, 2020, **15**, 100254.
31 T. Wang, W. Chen, T. Dong, Z. Lv, S. Zheng, X. Cao, Q. Wei, R. A. Ghiladi and Q. Wang, *Materials*, 2020, **13**, 4141.
32 X. Nie, S. Wu, A. Mensah, Q. Wang, F. Huang, D. Li and Q. Wei, *J. Colloid Interface Sci.*, 2020, **579**, 233–242.
33 P. Tang, Z. Zhang, A. Y. El-Moghazy, N. Wisuthiphaet, N. Nitin and G. Sun, *ACS Appl. Mater. Interfaces*, 2020, **12**, 49442–49451.
34 J. Kim and S. Michielsen, *Nanomaterials*, 2016, **6**, 243.
35 D. Khaki, H. Namazi and S. M. Amininasab, *React. Funct. Polym.*, 2021, **158**, 104780.
36 B. L. Deopura, *Polyesters and Polyamides*, Elsevier, 2008, pp. 41–61.
37 N. Vasanthan, *Handbook of Textile Fibre Structure*, Elsevier, 2009, pp. 232–256.
38 Y. Son and G. Sun, *J. Appl. Polym. Sci.*, 2003, **90**, 2194–2199.
39 N. Sekar, *Handbook of Textile and Industrial Dyeing*, Elsevier, 2011, pp. 486–514.
40 M. A. Saleem, L. Pei, M. F. Saleem, S. Shahid and J. Wang, *Text. Res. J.*, 2023, **93**, 554–564.
41 R. Gavara, R. de Llanos, V. Pérez-Laguna, C. Arnau del Valle, J. F. Miravet, A. Rezusta and F. Galindo, *Front. Med.*, 2021, **8**, 641646.
42 N. Mori, H. Kawasaki, E. Nishida, Y. Kanemoto, H. Miyaji, J. Umeda and K. Kondoh, *J. Mater. Sci.*, 2023, **58**, 2801–2813.
43 T. Wright, M. Vlok, T. Shapira, A. D. Olmstead, F. Jean and M. O. Wolf, *ACS Appl. Mater. Interfaces*, 2022, **14**, 49–56.
44 C. R. Ghareeb, B. S. T. Peddinti, S. C. Kisthardt, F. Scholle, R. J. Spontak and R. A. Ghiladi, *Front. Med.*, 2021, **8**, 657837.
45 D. Hillel, *Environmental Soil Physics*, Academic Press, London, 1998.
46 N. Nasri, A. Rusli, N. Teramoto, M. Jaafar, K. M. Ku Ishak, M. D. Shafiq and Z. A. Abdul Hamid, *Polymers*, 2021, **13**, 4234.
47 M. M. Azevedo, P. Ramalho, A. P. Silva, R. Teixeira-Santos, C. Pina-Vaz and A. G. Rodrigues, *J. Med. Microbiol.*, 2014, **63**, 1167–1173.
48 A. Minnock, D. I. Vernon, J. Schofield, J. Griffiths, J. Howard Parish and S. B. Brown, *J. Photochem. Photobiol., B*, 1996, **32**, 159–164.
49 C. Vera, M. N. Gallucci, J. Marioni, M. C. Sosa Morales, D. M. Martino, S. Nuñez Montoya and C. D. Borsarelli, *Bioconjug. Chem.*, 2022, **33**, 463–472.
50 E. Fuentes-Lemus, M. Mariotti, P. Hägglund, F. Leinisch, A. Fierro, E. Silva, C. López-Alarcón and M. J. Davies, *Free Radical Biol. Med.*, 2019, **143**, 375–386.
51 S. Criado, S. G. Bertolotti and N. A. García, *J. Photochem. Photobiol., B*, 1996, **34**, 79–86.
52 F. Sperandio, Y.-Y. Huang and M. Hamblin, *Recent Pat. Antiinfect. Drug Discovery*, 2013, **8**, 108–120.
53 B. Barrios, B. Mohrhardt, P. V. Doskey and D. Minakata, *Environ. Sci. Technol.*, 2021, **55**, 8054–8067.
54 W. Xiang, Z. Xiaoshen, S. Grzegorz, E.-H. Ahmed, H. Ying-Ying, S. Tadeusz and M. R. Hamblin., *Antimicrob. Agents Chemother.*, 2017, **61**, e00467–17.
55 R. F. Donnelly, P. A. McCarron, M. M. Tunney and A. David Woolfson, *J. Photochem. Photobiol., B*, 2007, **86**, 59–69.

56 C. K. L. Ng, D. Obando, F. Widmer, L. C. Wright, T. C. Sorrell and K. A. Jolliffe, *J. Med. Chem.*, 2006, **49**, 811–816.
57 G. Zhu, A. G. Nicolson, X.-X. Zheng, T. B. Strom and V. P. Sukhatme, *Kidney Int.*, 1997, **52**, 992–999.
58 T. Bayraktutan, *Chem. Pap.*, 2020, **74**, 3017–3024.
59 M. A. Rauf, J. P. Graham, S. B. Bukallah and M. A. S. Al-Saedi, *Spectrochim. Acta, Part A*, 2009, **72**, 133–137.
60 C. R. Lambert and I. E. Kochevar, *Photochem. Photobiol.*, 1997, **66**, 15–25.
61 S. D.-M. Islam and O. Ito, *J. Photochem. Photobiol., A*, 1999, **123**, 53–59.

